nature nanotechnology

LETTERS

PUBLISHED ONLINE: 23 AUGUST 2009 | DOI: 10.1038/NNANO.2009.233

Single-crystal germanium layers grown on silicon by nanowire seeding

Shu Hu[1], Paul W. Leu[2], Ann F. Marshall[3] and Paul C. McIntyre[1,3]*

Three-dimensional integration and the combination of different material systems are central themes of electronics research. Recently, as-grown vertical one-dimensional structures have been integrated into high-density three-dimensional circuits. However, little attention has been paid to the unique structural properties of germanium nanowires obtained by epitaxial and heteroepitaxial growth on Ge(111) and Si(111) substrates[1,2], despite the fact that the integration of germanium on silicon is attractive for device applications. Here, we demonstrate the lateral growth of single crystal germanium islands tens of micrometres in diameter by seeding from germanium nanowires grown on a silicon substrate. Vertically aligned high-aspect-ratio nanowires can transfer the orientation and perfection of the substrate crystal to overlying layers a micrometre or more above the substrate surface. This technique can be repeated to build multiple active device layers, a key requirement for the fabrication of densely interconnected three-dimensional integrated circuits.

Germanium layers heterogeneously integrated on silicon are interesting for transistor applications because germanium has large intrinsic electron and hole mobilities[3]. Recent work on surface passivation of planar germanium surfaces with high-dielectric-constant materials[4,5] has enabled germanium integration in silicon-based semiconductor circuits. There is also great interest in the integration of germanium on silicon substrates to enable on-chip opto-electronics[6]. Also, germanium has good lattice matching with III–V semiconductors (such as GaAs), and it can therefore be used as a buffer layer for the integration of III–V materials on silicon. Selective etching of via holes and via-filling deposition (by electrodeposition, collimated sputtering, and so on) can be used to make metallic electrical interconnects between device layers. For three-dimensional devices and integrated circuits, such connections are necessary, and programmable vertical interconnects are particularly advantageous. Germanium nanowire vertical pn junctions connecting adjacent device layers are desirable, for example, as memory-cell selection devices for high-density crosspoint memory[7].

Several techniques have been pursued to obtain single-crystal germanium above a silicon layer, including rapid melt growth[8], solid-phase crystallization[9], selective oxidation of silicon from SiGe alloy films[10] and laser annealing. Localized laser radiation can control the thermal budget for fabricating surface layers, without damaging underlying temperature-sensitive devices and interconnects[11]. The relatively low growth temperature (<400 °C) for germanium nanowires[2,12] makes them compatible with the fabrication of three-dimensional integrated circuits. Although the present demonstration of germanium nanowire seeded crystallization uses rapid thermal annealing to heat germanium crystals on oxide-coated silicon substrates, it is also suitable for laser thermal processing methods.

Figure 1 shows scanning electron microscopy (SEM) images at various stages in fabrication. Using the two-temperature vapour–liquid–solid (VLS) growth method[1,2], germanium nanowires were grown heteroepitaxially from the Si(111) surface with a strong preference for vertical epitaxial growth and no detectable tapering (Fig. 1a). Catalyst particles were randomly deposited by a dip-coating method with an areal density of $\sim$0.3–0.5 μm^{-2} on the silicon surface. Vertically aligned nanowires were then encapsulated in SiO_2 to provide structural support. Chemical mechanical polishing (CMP) was used to planarize the surface, so that the polished surface[13] became the substrate for the second semiconductor layer. An amorphous-germanium (*a*-Ge) thin film was then deposited by electron-beam evaporation, with film thicknesses of 30 nm to 1 μm investigated. Figure 1c shows an array of 30×30 μm germanium islands after photolithography and a lift-off process, followed by SiO_2 cap layer deposition. The area of the patterned islands ensures that at least one germanium nanowire is in contact with each island. The cap layer and the underlying planarized oxide surface were used to prevent germanium liquid from flowing and to avoid local germanium dewetting during annealing. Finally, after crystallization and subsequent cap layer removal, vertically aligned germanium nanowires were grown for a second time with the same process on annealed germanium islands (Fig. 1d), confirming the islands' single-crystalline structure after optimized thermal anneals.

Transmission electron microscopy (TEM) was used to characterize the crystallized germanium islands after thermal processes. The samples were heated by rapid thermal annealing (RTA) to temperatures in the range of $\sim$900–940 °C. The upper end of this temperature range is similar to the bulk germanium melting point, $T_m = 937$ °C. First, we investigated germanium islands crystallized through attempted lateral solid-phase epitaxy (SPE—crystallization performed without melting the *a*-Ge island). Structures similar to those shown in Fig. 1 were polished from the substrate side during plan-view TEM specimen preparation. Selected-area electron diffraction (SAED) patterns taken before annealing show no sharp diffraction features among diffuse rings, indicating that the as-deposited germanium films are amorphous. During the SPE anneals, the temperature was increased from room temperature to 900 °C in 25 s, and held for 5 s. The diffraction ring pattern of the diamond cubic crystal structure (Fig. 2a inset) from the germanium region indicates that the crystallized islands exhibit a polycrystalline germanium (*poly*-Ge) structure after SPE anneal: the crystallites have random orientations distributed across each germanium island. The average grain size ($\sim$30 nm) in the *poly*-Ge islands depicted in Fig. 2a is similar to the *a*-Ge film thickness of this sample. Epitaxially aligned germanium crystallites found in the vicinity of the contact points with germanium nanowire tips were apparently seeded from the germanium nanowire (white dashed circle). These epitaxial crystallites impinge upon other randomly oriented crystallites that nucleated elsewhere.

[1]Department of Materials Science and Engineering, Stanford University, Stanford, California 94305, USA, [2]Department of Mechanical Engineering, Stanford University, Stanford, California 94305, USA, [3]Geballe Laboratory for Advanced Materials, Stanford University, Stanford, California 94305, USA. *e-mail: pcm1@stanford.edu

© 2009 Macmillan Publishers Limited. All rights reserved.

NATURE NANOTECHNOLOGY DOI: 10.1038/NNANO.2009.233

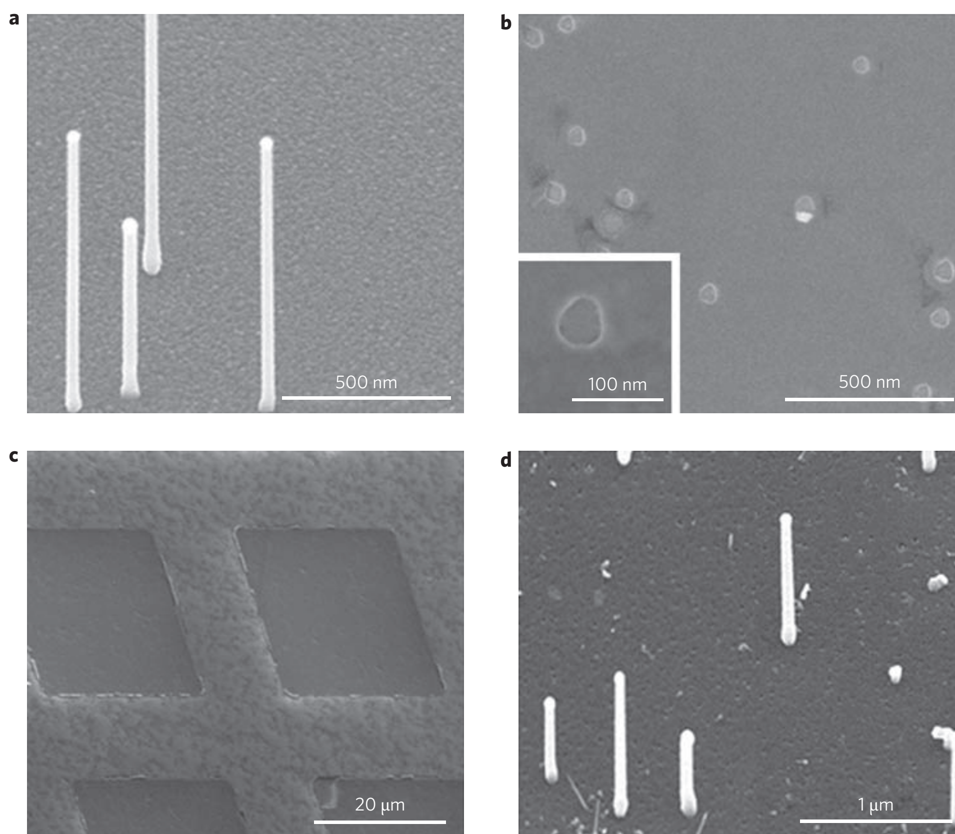

Figure 1 | SEM micrographs of the samples at various points in the processing sequence. **a**, 45° from plan-view image of germanium nanowires on a (111) silicon substrate. **b**, Plan-view SEM image of as-exposed germanium nanowire tips after the CMP process. The inset shows the top view of one polished nanowire. **c**, 45° from plan-view image of germanium islands before annealing. **d**, 45° from plan-view image of germanium nanowire CVD growth under the same conditions as in **a** on one crystallized germanium island.

The observations imply that SPE annealing at 900 °C makes nanowire-seeded epitaxial crystallization of an entire germanium island highly improbable. This is consistent with the findings of an *in situ* TEM heating study (results not shown) that indicate that large numbers of random nuclei form at temperatures below 700 °C, producing the same poly-crystallinity as seen in Fig. 2a.

Liquid phase epitaxy (LPE) has the potential to grow thin germanium crystals of much larger lateral size[8]. Compared to the SPE anneal process, the maximum temperature in the present experiments was increased to 940 °C (with the same ramping rate from room temperature) and was held at that temperature for 2 s. TEM bright-field images (Fig. 2b) depict the germanium island after crystallization from the liquid. The inset of Fig. 2b shows that the LPE-annealed germanium island is a single crystal (*c*-Ge), as indicated by the presence of discrete 220 and 422 type reflections in the SAED pattern. This pattern is consistent with [111] zone axis parallel to the surface normal of the Si(111) wafer. The results show a substantial difference in crystallization kinetics for the SPE and LPE anneals, with a relatively small difference in maximum annealing temperature (900 °C versus 940 °C). After anneals, the split reflections observed in the enlarged SAED pattern (Fig. 2b, inset) show that both the germanium and silicon crystals are well aligned, with the same $2\bar{2}0$, $20\bar{2}$ and $4\bar{2}\bar{2}$ in-plane orientations, an indicator of seeded epitaxial crystallization. Cross-section TEM analysis (Fig. 2c,d) confirms the crystallinity of LPE-grown germanium islands. Crystallized germanium islands are effectively encapsulated in oxide micro-crucibles after thermal processing without any evidence of gap formation between the crucibles and the germanium islands. The light contrast region near a germanium nanowire in both plan-view and cross-section TEM micrographs results from local variations in oxide density of the PECVD SiO_2 encapsulation after CMP and wet cleaning processes[13]. A larger area investigation (Fig. 2c) suggests the SiO_2 encapsulation density variation near the nanowire has little effect on the crystallinity of the annealed germanium islands.

Electron back-scattered diffraction (EBSD) was used to investigate the LPE-grown germanium crystals over larger areas. Figure 3 shows the SEM micrograph and corresponding EBSD germanium orientation map of a representative nanowire-seeded, LPE-grown germanium island. The blue region in Fig. 3b shows uniform Ge[111] azimuthal orientation over the entire island, whereas the region with varying colours is the polished silica surface. The EBSD results confirm that the tens of micrometre-scale LPE growth regions seeded by germanium nanowires are large-area single crystals grown above the silicon wafer surface.

Resistivities of SPE- and LPE-annealed, undoped germanium islands were compared to determine the effects of microstructure on the properties of the crystallized germanium layers. Electrical measurements were carried out with probe tips made of copper–beryllium alloy, forming ohmic contacts at two opposite corners of the germanium island. The germanium film thickness for both types of islands was 100 nm. The in-plane conductance (Fig. 4) of nanowire-seeded LPE germanium single crystals (labelled with open triangles) is almost two orders of magnitude less than that of *poly*-Ge (labelled with filled squares) at a given bias. The larger current through the SPE-annealed polycrystalline germanium islands suggests local leakage current paths along grain boundaries, which have numerous defect states[14,15]. The relatively small leakage current observed for the LPE germanium islands is consistent with their single-crystalline structure.

For seeded crystallization to grow large-area single-crystal films from an initially liquid or amorphous state, there are two

© 2009 Macmillan Publishers Limited. All rights reserved.

Figure 2 | TEM micrographs of crystallized germanium islands. a, Plan-view bright-field image of *poly*-Ge film after a 900 °C anneal, with a SAED pattern from the area of interest shown in the inset. The film thickness of the germanium islands in these images is 30 nm. **b**, Plan-view bright-field image of crystallized germanium islands in contact with the underlying germanium nanowires after a 940 °C anneal. The lower inset is the SAED pattern on [111] zone axis, and the upper inset is an enlarged version showing split diffraction spots. The film thickness is 100 nm. **c**, Nanowire-seeded LPE germanium island cross-section. The island thickness is 1 μm. **d**, Typical structure of nanowire-seeded regions (a portion of one LPE-grown *c*-Ge island), as well as a microdiffraction pattern taken in the vicinity of the germanium nanowire and LPE germanium island.

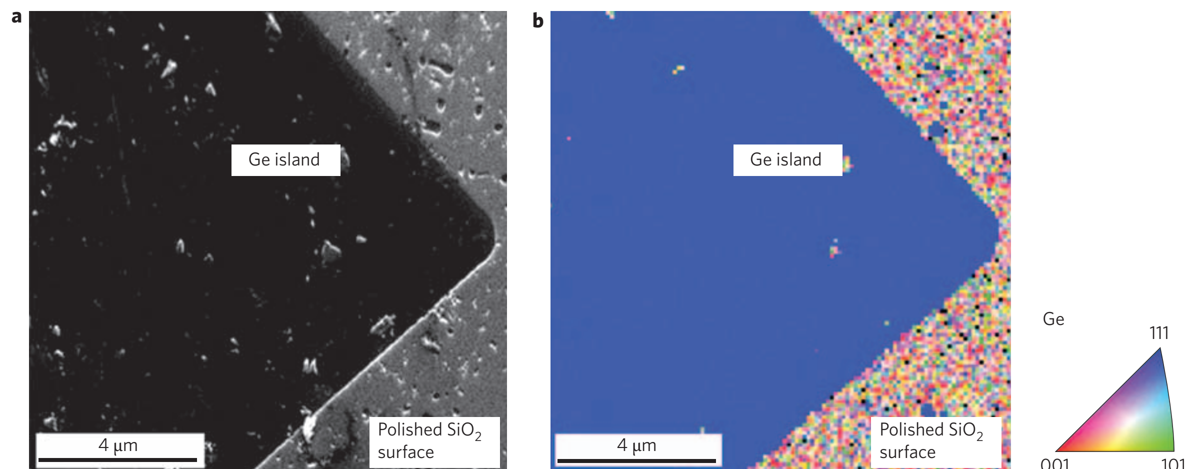

Figure 3 | EBSD analysis of a 30 μm × 30 μm germanium island after LPE. a, Plan-view SEM image of the crystallized germanium island. **b**, EBSD germanium orientation mapping, with the inset showing a germanium inverse pole figure as a legend.

© 2009 Macmillan Publishers Limited. All rights reserved.

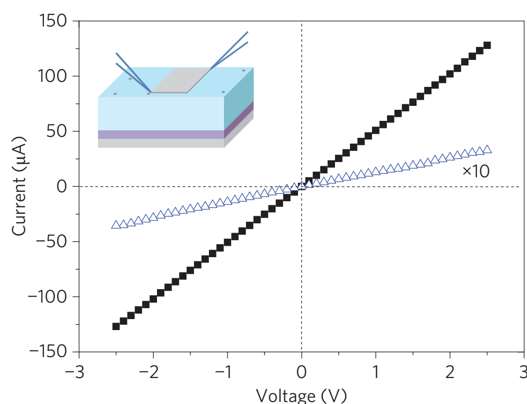

Figure 4 | In-plane electrical measurements of crystallized germanium islands (100 nm thick), with crystallization processes as described in Fig. 2a and b, respectively. The curve labelled with solid squares is for SPE germanium, and triangles for LPE germanium (multiplied by a factor of 10).

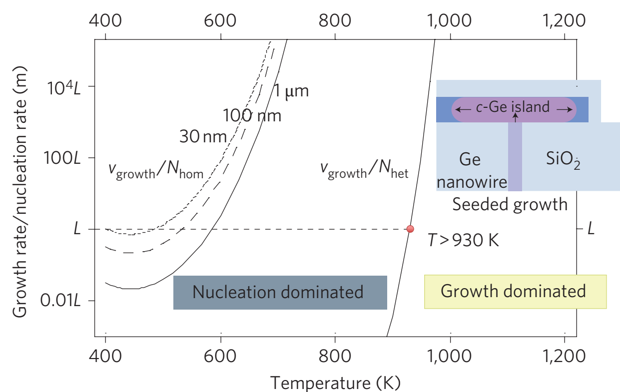

Figure 5 | Estimated growth velocity scaled by homogeneous and heterogeneous nucleation rate versus temperature for a 30 μm × 30 μm germanium island with thin-film thicknesses of 30 nm, 100 nm and 1 μm encapsulated in SiO_2. Inset: schematic drawing for LPE growth of the germanium island seeded from a germanium nanowire, in the growth-dominated temperature window.

requirements: during the thermal process, any emerging or existing *poly*-Ge grains are eliminated by transient melting, for example, LPE; and the seeded crystallization happens in a temperature window where the growth front propagates sufficiently quickly to occlude unseeded nucleation sites in the region of interest. The temperature for successful LPE growth is similar to the melting point of bulk crystalline germanium. This is substantially higher than the melting point of 970 K (∼700 °C) for *a*-Ge calculated previously[16]. SPE-annealed films indicate that uncontrolled nucleation occurs during heating up at temperatures below the *a*-Ge melting point. Given the relatively high maximum annealing temperature (940 °C) in LPE experiments, patterned germanium islands are likely to be completely melted from a *poly*-Ge state.

As the temperature decreases rapidly at the end of RTA (at a rate of ∼100 °C s^{-1}), epitaxial growth of crystalline-Ge (*c*-Ge) seeded by the nanowires occurs as the *c*-Ge/liquid-Ge (*l*-Ge) interface sweeps across the undercooled *l*-Ge layer (Fig. 5, inset). To understand the formation of relatively large single-crystal germanium islands, we estimated the temperature dependence of both the crystal growth velocity and nucleation rates for germanium islands with various thicknesses using a method as previously reported by Liu *et al.*[8]. The estimation procedure is described in the Methods. The lateral crystal growth velocity v_{growth} was compared to the nucleation rate (s^{-1}) within a 30 μm × 30 μm germanium island. Both homogeneous and heterogeneous nucleation rates (N_{hom} and N_{het}) were considered. The experimental results suggest that *l*-Ge solidification during the LPE process is completed in the temperature window where $v_{growth}/N_{het} > L$ (here, L is the germanium island lateral dimension), as shown in Fig. 5. The homogeneous nucleation rate is related to the overall island volume, and is less than the heterogeneous nucleation rate for film thicknesses of 30 nm, 100 nm and 1 μm investigated experimentally. Therefore, crystallization in LPE experiments is governed by a competition between heterogeneous nucleation and lateral crystal growth of germanium from the nanowire seeds.

Our results, which show a dramatic change in crystallized germanium island structure from polycrystalline to large-area single crystals by increasing the maximum RTA temperature from 900 °C to 940 °C, indicate that island melting occurs at temperatures near the bulk germanium melting point. This is not unexpected, given the relatively large island diameters and thicknesses we have studied. Others[17] have reported a large melting point hysteresis for much smaller germanium nanocrystals (∼5 nm diameter) embedded in SiO_2. However, the much smaller surface area-to-volume ratio of our germanium islands greatly reduces the effect of interface energy on their melting behaviour, consistent with the observation of bulk-like polycrystalline germanium melting temperature.

In conclusion, we have demonstrated a method to obtain crystalline germanium islands on a scale of tens of micrometres on amorphous silica substrates by lateral LPE from vertical germanium nanowire seeds. The crystallization seeds are provided by vertically aligned ⟨111⟩ germanium nanowires encapsulated in PECVD-deposited silica after the heteroepitaxial growth of germanium nanowires on a silicon substrate. The location of the islands above the silicon surface is dictated by chemical mechanical planarization of the SiO_2 encapsulation, and can be varied over a wide range. Liquid phase epitaxy during cooling from temperatures near the bulk germanium melting point was found to produce single crystal islands, whereas lower temperature, solid-phase epitaxy anneals resulted in polycrystalline films in which random nucleation competed with germanium lateral growth from nanowire seeds. Other than the annealing step, all processes took place at temperatures below 400 °C. Given a low thermal budget annealing process, such as laser annealing[11], nanowire-seeded lateral crystallization is a promising approach for monolithic three-dimensional integration of large-area single-crystalline semiconductor layers on top of silicon.

Methods

Fabrication of Ge nanostructures. We used p-type boron-doped (111) silicon with resistivity ranging from 8.0 to 20.0 Ω cm as the substrate. A standard RCA cleaning method was used to remove hydrocarbon contaminants, leaving an H-terminated silicon surface. A 10:1 mixture of colloidal gold particle (BB International, nominal particle diameter 40 nm) solution and diluted 2% HF/deionized water solution[2] was applied to the silicon surface for 30 s to deposit catalyst by dip-coating. Nanowire growth was carried out in a cold-wall, lamp-heated chemical vapour deposition (CVD) chamber, with a germane precursor flow of 10 s.c.c.m., H_2 flow of 490 s.c.c.m., and a total pressure of 30 torr. The substrates were heated to 375 °C for a nucleation step of 2 min, and then cooled within 30 s to 300 °C where nanowires grew for 12 min. Plasma-enhanced CVD silica (700 nm thick) encapsulated both inclined and vertical nanowires, with a gas mix of 2% silane diluted in nitrogen (flow rate 400 s.c.c.m.) and nitrous oxide (flow rate 1,400 s.c.c.m.), a total pressure of 650 mtorr, and a deposition temperature of 350 °C with 40 W power at radio frequency 13.56 MHz. After the CMP process[13], inclined ⟨111⟩ -oriented germanium nanowires were buried well below the as-polished surface. Amorphous germanium thin films were deposited in an electron-beam evaporation system. The thickness of germanium thin-film islands ranged from 30 nm to 1 μm.

Characterization. Annealing was carried out in a commercial rapid thermal processing (RTP) furnace (thermal couple temperature accuracy ±2 °C). The samples were subsequently cooled in an argon atmosphere with an initial rate 100 °C s^{-1}. A well-controlled 2% HF etching was then used to remove the cap layer. SEM and EBSD characterization was carried out with an FEI XL30 Sirion SEM with a commercial TSL EBSD system. Plan-view TEM specimens were thinned from the silicon backside by polishing and low-energy ion milling, and were then characterized with a Philips CM20 at 200 kV. In-plane conductivity measurement was carried out in a two-probe station, with probe tips made of copper–beryllium

© 2009 Macmillan Publishers Limited. All rights reserved.

alloy and a contact point radius of 1 μm. A computer-programmed voltage source applied bias between the probe tips, which formed ohmic contacts with very low contact resistance at two opposite corners of the germanium island. The voltage across the germanium island was well defined by the applied bias. The current through the two probes was measured by a current meter and recorded automatically.

Nucleation and growth rate calculation. We define I_{hom} as the homogeneous nucleation frequency per unit volume ($s^{-1}\,cm^{-3}$) and I_{het} as the heterogeneous nucleation frequency per unit l-Ge/SiO_2 interface area ($s^{-1}\,cm^{-2}$). Consider v_{growth} as the l/c-Ge interface propagation velocity during LPE. We assume no atomic volume (V_m) change during crystallization, no change in the geometry of the islands (lateral length L and layer thickness h), spherical curvature of the nucleus surface for both homo- and heterogeneous nucleation, and that the attempt frequencies ν_0 and the energy barriers $\Delta G'_M$ for atom motion across the liquid–nucleus interface and liquid–crystal interface are the same. The heat dissipation rate from l-Ge to the substrate is assumed to be fast enough that the liquid–crystal interface velocity is governed by atomic motion. From classical nucleation theory[18–21]

$$I_{hom} = \frac{1}{V_m^{2/3}}\nu_0 \exp\left(-\frac{\Delta G'_M}{kT}\right)4\pi(r^*)^2\frac{1}{V_m n^*_{hom}} \times \left(\frac{\Delta G^*_{hom}}{3\pi kT}\right)^{1/2}\exp\left(-\frac{\Delta G^*_{hom}}{kT}\right) \quad (1)$$

$$I_{het} = \frac{1}{V_m^{2/3}}\nu_0 \exp\left(-\frac{\Delta G'_M}{kT}\right)2\pi(r^*)^2(1-\cos\theta)\frac{1}{V_m^{2/3} n^*_{het}} \times \left(\frac{\Delta G^*_{het}}{3\pi kT}\right)^{1/2}\exp\left(-\frac{\Delta G^*_{het}}{kT}\right) \quad (2)$$

$$v_{growth} = a_0\nu_0\exp\left(-\frac{\Delta G'_M}{kT}\right)\left[\exp\left(\frac{\Delta g_N}{2kT}\right)-\exp\left(-\frac{\Delta g_N}{2kT}\right)\right] \quad (3)$$

where T is the temperature, r^* is the critical nuclei radius in the undercooled liquid, a_0 is the interatomic spacing, Δg_N is the driving force per atom from l-Ge to c-Ge: the free energy change is calculated from the enthalpy and entropy of l-Ge and c-Ge at the melting point using their respective specific heat values, C_p (ref. 22). ΔG^*_{hom} and ΔG^*_{het} are the homogeneous and heterogeneous nucleation barriers, respectively, and n^*_{hom} and n^*_{het} are the number of atoms in a critically sized nucleus for homogeneous and heterogeneous nucleation:

$$\Delta G^*_{het} = \Delta G^*_{hom}S(\theta),\ n^*_{het} = n^*_{hom}S(\theta) \quad (4)$$

where $S(\theta) = (2+\cos\theta)(1-\cos\theta)^2/4$ and θ is the contact angle of germanium nuclei with the undercooled liquid and germanium/SiO_2 interface. The radius r^* of critically sized homogeneous nuclei is given by $2\gamma_{SL}V_m/\Delta g_N$, and the energy barrier to form a critically sized nucleus is $\Delta G^*_{hom} = 16\pi\gamma_{SL}^3V_m^2/3\Delta g_N^2$, where $\gamma_S L$ is the liquid/c-Ge interface energy. Given a germanium island with area L^2 and thickness h, the homogeneous nucleation rate is $N_{hom} = I_{hom}L^2h$, whereas the heterogeneous nucleation rate is $N_{het} = I_{het}(2L^2)$. The other constants are given as $V_m = 4.4\times10^{-22}\,cm^3$, $\nu_0 = 1.12\times10^{13}$ Hz, $\Delta G'_M = 0.332$ eV $= 5.31\times10^{-20}$ J/atom (ref. 23) and γ_{SL} is calculated as 0.334 J m^{-2} (ref. 24). The contact angle $\theta = 72^\circ$ was estimated by Liu *et al.*[8], based on Turnbull's solidification experiments with l-Ge on a quartz surface. Finally, v_{growth}/N_{hom} and v_{growth}/N_{het} are normalized by dimensions of germanium islands for comparison in Fig. 5.

Received 5 June 2009; accepted 14 July 2009; published online 23 August 2009

References

1. Adhikari, H., Marshall, A. F., Chidsey, C. E. D. & McIntyre, P. C. Germanium nanowire epitaxy: shape and orientation control. *Nano Lett.* **6,** 318–323 (2006).
2. Jagannathan, H. *et al.* Nature of germanium nanowire heteroepitaxy on silicon substrates. *J. Appl. Phys.* **100,** 024318 (2006).
3. Shang, H. *et al.* Electrical characterization of germanium *p*-channel MOSFETs. *IEEE Electron. Dev. Lett.* **24,** 242–244 (2003).
4. Chui, C. O. *et al.* Germanium MOS capacitors incorporating ultrathin high-kappa gate dielectric. *IEEE Electron. Dev. Lett.* **23,** 473–475 (2002).
5. Kim, H., Chui, C. O., Saraswat, K. C. & McIntyre, P. C. Local epitaxial growth of ZrO2 on Ge(100) substrates by atomic layer epitaxy. *Appl. Phys. Lett.* **83,** 2647–2649 (2003).
6. Okyay, A. K. *et al.* High-efficiency metal–semiconductor–metal photodetectors on heteroepitaxially grown Ge on Si. *Opt. Lett.* **31,** 2565–2567 (2006).
7. Kim, S. *et al.* Integrating phase-change memory cell with Ge nanowire diode for crosspoint memory-experimental demonstration and analysis. *IEEE Trans. Electron. Dev.* **55,** 2307–2313 (2008).
8. Liu, Y. C., Deal, M. D. & Plummer, J. D. Rapid melt growth of germanium crystals with self-aligned microcrucibles on si substrates. *J. Electrochem. Soc.* **152,** G688–G693 (2005).
9. Csepregi, L., Kennedy, E. F., Mayer, J. W. & Sigmon, T. W. Substrate-orientation dependence of epitaxial regrowth rate from Si-implanted amorphous Si. *J. Appl. Phys.* **49,** 3906–3911 (1978).
10. Nakaharai, S. *et al.* Characterization of 7-nm-thick strained Ge-on-insulator layer fabricated by Ge-condensation technique. *Appl. Phys. Lett.* **83,** 3516–3518 (2003).
11. Witte, D. J. *et al.* Lamellar crystallization of silicon for 3-dimensional integration. *Microelectron. Eng.* **84,** 1186–1189 (2007).
12. Kodambaka, S., Tersoff, J., Reuter, M. C. & Ross, F. M. Germanium nanowire growth below the eutectic temperature. *Science* **316,** 729–732 (2007).
13. Leu, P. W. *et al.* Oxide-encapsulated vertical germanium nanowire structures and their dc transport properties. *Nanotechnology* **19,** 485705 (2008).
14. Fossum, J. G., Ortizconde, A., Shichijo, H. & Banerjee, S. K. Anomalous leakage current in LPCVD polysilicon MOSFETs. *IEEE Trans. Electron. Dev.* **32,** 1878–1884 (1985).
15. Ahmed, S., Kim, D. & Shichijo, H. A comprehensive analytic model of accumulation-mode MOSFETs in polysilicon thin films. *IEEE Trans. Electron. Dev.* **33,** 973–985 (1986).
16. Spaepen, F. & Turnbull, D. Kinetics of motion of crystal–melt interfaces. *AIP Conf. Proc.* **50,** 73–83 (1979).
17. Xu, Q. *et al.* Large melting-point hysteresis of Ge nanocrystals embedded in SiO_2. *Phys. Rev. Lett.* **97,** 155701 (2006).
18. Turnbull, D. & Fisher, J. C. Rate of nucleation in condensed systems. *J. Chem. Phys.* **17,** 71–73 (1949).
19. Turnbull, D. Kinetics of heterogeneous nucleation. *J. Chem. Phys.* **18,** 198–203 (1950).
20. Turnbull, D. & Cohen, M. H. Concerning reconstructive transformation and formation of glass. *J. Chem. Phys.* **29,** 1049–1054 (1958).
21. Becker, R. & Doring, W. Kinetische behandlung der keimbildung in ubersattigten dampfen. *Ann. Phys.-Berlin* **24,** 719–752 (1935).
22. Lide, D. R. *CRC Handbook of Chemistry and Physics* (Taylor and Francis, 2008).
23. Stojic, M., Babic Stojic, B. & Milivojevic, D. Influence of vacancies on the static and dynamic properties of monoatomic liquids. *Phys. B: Condens. Matter* **334,** 274–286 (2003).
24. Evans, P. V., Devaud, G., Kelly, T. F. & Kim, Y.-W. Solidification of highly undercooled Si and Ge droplets. *Acta Metall. Mater.* **38,** 719–726 (1990).

Acknowledgements

The authors thank the members of the Nanowire Facility at Stanford University, I. A. Goldthorpe, J. Ratchford, J. Woodruff, Y. Zhang and H. Adhikari for helping maintain the nanowire growth reactor, and J. McVittie and Y. Nishi for managing the facility. The authors also thank T. Brand and R. Macdonald for help in the CMP process and J. Feng for useful discussions. Funding for this work was provided by the DARPA SPAWAR 3D-IC programme, a Stanford School of Engineering Fellowship and a Stanford Graduate Fellowship.

Author contributions

All authors discussed the results and commented on the manuscript. S.H. and P.C.M. conceived and designed the experiments, analysed the data and co-wrote the paper. S.H. and P.W.L. performed the experiments. A.F.M. contributed TEM sample preparation and analysis.

Additional information

Reprints and permission information is available online at http://npg.nature.com/reprintsandpermissions/. Correspondence and requests for materials should be addressed to P.C.M.

© 2009 Macmillan Publishers Limited. All rights reserved.